Article citation info:
Socik P, Zadrąg R, Zacharewicz M, Bogdanowicz A, Kniaziewicz T, Wirkowski P et al. Seasonal environmental assessment of PEMFC/BOP components in a ship hybrid propulsion system under Baltic Sea and North Sea conditions. Combustion Engines. 0000;XXX(X):xx-xx. https://doi.org/10.19206/CE-236173

Paweł SOCIK
Ryszard ZADRĄG
Marcin ZACHAREWICZ
Artur BOGDANOWICZ
Tomasz KNIAZIEWICZ
Paweł WIRKOWSKI
Adriana WŁÓKA

Combustion Engines
Polish Scientific Society of Combustion Engines

Seasonal environmental assessment of PEMFC/BOP components in a ship hybrid propulsion system under Baltic Sea and North Sea conditions

ARTICLE INFO

Received: 5 May 2026
Revised: 11 August 2026
Accepted: 8 September 2026
Available online: 25 September 2026

This paper presents an analysis of the impact of the marine environment on selected components of a ship hybrid propulsion system, including the PEMFC/BOP section (balance-of-plant auxiliary equipment), structural elements, joints and mountings. The analysis was carried out for Baltic Sea conditions, with four seasons, two exposure levels and North Sea reference scenarios with high chloride deposition. Four mutually complementary assessment areas were considered: thermal-moisture, corrosion, electrochemical and dynamic effects. The thermal-moisture part was described using a heat balance and the dew point. Corrosion effects were determined from chloride deposition S_d and the ISO 9223 dose-response function. The PEM electrochemical part was represented using the Springer relations and the Tafel equation, whereas the dynamic part was described using the JONSWAP spectrum, the RAO operator and the rms acceleration a_{rms}. The scenarios were compared using the proposed decision metric R. The results indicate that the total environmental load results from the simultaneous influence of condensation, corrosion, electrochemical loading and dynamics, with individual mechanisms dominating under different operating conditions. In particular, two main sources of risk were separated: a humid-salt environment, which intensifies corrosion processes, and dry conditions, which reduce membrane hydration and increase the electrochemical load of the FC section. The study also shows that appropriately selected protective measures and changes in system configuration can significantly reduce the overall environmental impact in terms of corrosion, dynamic and electrochemical loads. The proposed approach may be used as a preliminary environmental qualification tool and as a basis for planning further validation tests.*

Key words: *PEMFC/BOP, hybrid propulsion, marine environment, JONSWAP, decision metric*

1. Introduction

Modernization of marine propulsion systems favours the increasingly common implementation of hybrid solutions, in which a conventional combustion source cooperates with energy storage systems, power converters and additional power sources, including fuel cells. In the present approach, the propulsion plant is treated not only as an internal combustion engine and its internal processes, but as an integrated set of interacting hybrid components. Consequently, the environmental conditions are assessed for the whole propulsion system, including the proton exchange membrane fuel cell (PEMFC) section, reformer, gas-preparation system, power converters, enclosures, joints, mountings and balance-of-plant (BOP) auxiliary equipment [5, 26, 27, 32, 34–36, 39, 43].

In marine applications, this assessment is particularly important. Moisture, salt aerosol, condensation, variable temperature, contamination of working media and dynamic loads act simultaneously on materials, joints, BOP elements and the operating conditions of the PEMFC section. They may cause corrosion of enclosures and fittings, increased flow resistance, sensor errors, local voltage losses, deterioration of membrane conductivity, loosening of connections and reduced readiness of the system to cover peak loads [8, 11–14, 25, 28, 36, 40, 42, 43].

The problem is important for naval vessels because their operating environment varies both seasonally and spatially. The Baltic Sea, which is the main operational area of the Polish Navy, has lower salinity than ocean waters, but it is characterized by large annual variability in temperature, humidity, icing, wind and sea state. Therefore, environmental qualification should not be based on a single averaged case. It requires a separation of seasons, exposure levels and storm situations, as well as a reference to the more aggressive North Sea conditions, which are also of operational interest to the Polish Navy [7, 15, 17, 18, 23, 31].

Previous studies show that marine PEMFC systems should be considered simultaneously as electrochemical, thermal-moisture and mechanical systems. Reviews of PEMFC use in shipping emphasize the importance of stack durability, BOP architecture, fuel and air quality, hydrogen safety and hybrid-system operating strategy [8, 10, 27, 39, 41]. Studies focused on salt aerosol show that salt ions may affect bipolar plates, the gas diffusion layer, the catalyst layer and the membrane, therefore, they are not only a problem of external enclosure corrosion [28, 40].

In the national literature, a useful interpretative basis is provided by the works of Dudek et al. concerning the design and testing of PEMFC stacks, operation in hybrid systems, air cooling and response to variable load [11–13]. From the naval-vessel perspective, important references also include studies on dynamic loads of propulsion systems [43], water content in fuels and lubricating oils of marine engines [42], and corrosion problems in shore-to-ship connections [25].

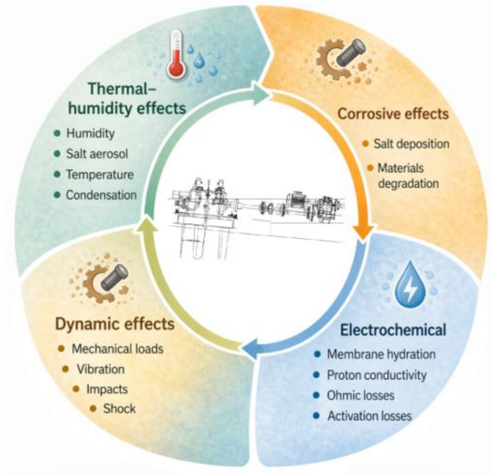

Fig. 1. Environmental factors affecting the propulsion system components

The aim of this paper is to assess the impact of seasonal environmental conditions on the PEMFC/BOP components of a ship hybrid propulsion system under Baltic Sea conditions, with reference to North Sea scenarios. A parametric approach was adopted, including eight Baltic scenarios and two North Sea scenarios. In addition, for comparison, a scenario with an environmental protection package was included. The analysis covers four seasons, two exposure levels and mechanisms linking temperature, humidity, chloride deposition and sea state with condensation, first-year corrosion loss, electrochemical loading of the PEMFC/BOP section and dynamic response.

2. Theoretical foundations and state of research

2.1. PEMFC/BOP in marine hybrid systems

PEMFCs are attractive for shipping because of their high conversion efficiency, low local emissions, modularity and ability to cooperate with batteries and conventional energy sources. In marine practice, however, the stack itself is not an autonomous power source. Its operation depends on the BOP, which includes hydrogen and air preparation, cooling, humidification, water separation, filtration, sensors, fittings, control and protection systems. Environmental qualification should therefore cover both the electrochemical section and the auxiliary elements and their connections [5, 10, 27, 32, 39, 41].

Available studies on hybrid systems indicate that the main implementation barriers are durability, cost, safety, integration with energy storage, control strategy and reliability under variable operating conditions [10, 33, 39, 41]. In a hybrid system, the PEMFC is usually not the only power source but rather an element that cooperates with batteries and power converters. This architecture reduces abrupt changes in stack load, but it increases the importance of proper BOP operation.

2.2. The impact of the humid-salt environment

The marine environment affects PEMFC/BOP systems primarily through the combined effects of moisture and salt. Marine aerosol can deposit on the surfaces of enclosures, connectors, air ducts and filtration elements. After dissolving in water, it creates conditions promoting corrosion and electrical leakage. In the electrochemical part, salt ions can affect the bipolar plates, the gas diffusion layer, the catalyst layer and the membrane, causing performance losses or increasing charge and mass transport resistances [28, 40].

The work by Li et al. systematizes the mechanisms by which salt spray affects PEMFCs and indicates that chlorides and other salt ions should be considered not only as corrosion agents but also as sources of internal stack contamination [28]. The experimental study by Wen et al. confirms that NaCl contamination can penetrate the membrane-electrode assembly and deteriorate performance under simulated salt-spray conditions [40]. For this reason, the present study separates the corrosion block, based on chloride deposition, from the PEM block, based on membrane hydration and electrochemical losses.

Condensation is another factor influencing system operation. Even at moderate salinity, a local exceedance of the dew point may cause prolonged wetting of connectors, cables, enclosures and air ducts. ISO 9223 addresses this aspect through the concept of time of wetness and atmospheric corrosivity classification, whereas ISO 9225 links assessment to measurements of environmental parameters, including chloride deposition S_d [20, 22]. This logic was used in the present analysis by adopting S_d as a scenario-based measure of chloride load.

2.3. Ship performance profiles and FC stack durability

The second group of factors comprises ship propulsion system load profiles. Unlike many stationary applications, a ship system operates with variable power demand, transitions between states, long periods of part load and potential shutdowns. Broer, Polinder and van Biert emphasize that PEMFC degradation in ships results from a combination of typical electrochemical mechanisms and marine-specific factors such as air salinity, ship motions, vibrations and load profiles [8].

Durability studies using ship operating profiles show that classical test protocols do not always represent real marine excitations. Choi et al. proposed a PEMFC durability test based on a ship operating profile, whereas McCay et al. tested a PEMFC stack for 1500 h under maritime-relevant conditions, distinguishing between reversible and irreversible degradation [9, 30]. Similarly, Tamburello et al. indicate that durability protocols should be tailored to the specific transport application because identifying the dominant stressors is a prerequisite for reliable lifetime assessment [38].

In special applications such as air-independent propulsion, additional stressors arise: high oxygen activity, longer dwell periods at high voltage, humidity and pressure transitions. Lim et al. show that such conditions may lead to MEA (membrane electrode assembly) failure modes that differ from those typical of land-based applications [29].

2.4. Validation and the research gap

Validation of environmental models requires combining environmental measurements with electrochemical and material diagnostics. The literature emphasizes the importance of polarization curves, EIS (electrochemical impedance spectroscopy), high-frequency resistance measurements, assessment of catalyst layers, membranes and bipolar plates, and post-mortem analyses [4, 28, 30, 40].

Bampaou et al. indicate that post-operation analysis enables the distinction between catalyst-layer degradation, membrane damage and the effects of contaminants. It is therefore a natural complement to bench tests [4].

The literature describes marine PEMFC architectures, salt-spray exposure, ship operating profiles, stack degradation and diagnostic methods mainly as separate issues. However, few studies integrate seasonal variations in temperature and humidity, condensation, chloride deposition, corrosion, electrochemical loading and mounting dynamics into a single framework. This study partially addresses this gap for special-purpose vessels. The proposed approach should be regarded as a preliminary qualification tool rather than a validated lifetime prediction model. Studies on marine PEMFC applications support the environmental interpretation, whereas standards and classical works on dew point, atmospheric corrosion, membrane conductivity, electrochemical kinetics and dynamic response provide the methodological basis for the individual modules, but do not directly validate the complete framework under marine conditions.

3. Environment model and methodology

3.1. Environmental conditions

The Baltic Sea is a brackish sea with a strong salinity gradient. According to HELCOM, surface salinity decreases from approximately 15-18 PSU at the entrance through the Sound to 7-8 PSU in the Baltic Proper and 0–2 PSU in the northern and eastern parts of the basin [17]. For the purposes of the present analysis, two representative Baltic levels were adopted: a coastal variant of 5.0-5.5 PSU and an open-sea variant of 7.0–7.2 PSU. The North Sea, considered in two scenarios, was adopted as a high-salinity reference environment (34.5 PSU).

The seasonal variability of the Baltic Sea temperature is as important as its brackish character. According to the literature, surface water temperature in the open Baltic Sea usually ranges from 15 to 20°C in summer, whereas in midwinter it falls slightly below 0°C [23]. Maximum ice cover usually occurs between January and March, and in severe winters, ice may extend far to the south [15]. This means that environmental qualification cannot rely on a single "average" marine case.

The importance of ambient temperature as a factor controlling transient processes is also confirmed by the work of Zimakowska-Laskowska et al., which shows a clear influence of thermal conditions on the cold-start phase [45]. Although that study concerns an internal combustion engine, its methodological meaning is useful here: at low temperatures, material condition, heating rate, local condensation and the transient moisture distribution in the machinery space should be assessed separately.

In the dynamic approach, two variants based on literature data were adopted. First, HELCOM observational data show that in the northern part of the Baltic Proper, a significant wave height of 7.8 m was recorded, while in the western part of this basin, strong summer storms can raise H_s to about 4.1 m [18]. Second, the event-based analysis by FMI (Finnish Meteorological Institute) indicates that in winter, in larger Baltic sub-basins, exceedance of H_s = 2.5 m occurs on average once a week, and exceedances of 4 m in the Baltic Proper occur on average 1–2 times per month in winter [7]. Therefore, the analyzed scenarios include sea states 0–7 and wind speeds of 0–28 m/s.

The RH (relative humidity) value was taken as the relative humidity of the local air in the compartment near the analyzed component, corresponding to the temperature $T_{air,loc} = T_{loc}$. It is not the external air humidity directly, but a scenario parameter describing the local thermal-moisture conditions around the device.

The dynamic and partly probabilistic approach is also consistent with the conclusions of Andrych-Zalewska et al., who showed that in propulsion systems operating outside steady-state conditions, operating parameters exhibit a clearly variable and partly random character [2, 3]. In a shipboard application, the hull is excited in six degrees of freedom (6DOF): surge, sway, heave, roll, pitch and yaw. Wind and sea state, therefore, generate not only wave-induced motions and accelerations, but also transient heel, rolling and pitching moments, vibrations of mounted equipment and fluctuating loads in connectors, brackets and auxiliary units. In the proposed model, this logic was extended to environmental excitations: wind and sea state are not treated as single numbers but as inputs that lead to motions, accelerations and mounting response.

Table 1. Literature basis for the Baltic environmental ranges

Range	Literature basis	Use in the model
Baltic Sea salinity	15-18 PSU at the entrance, 7-8 PSU in the Baltic Proper, and 0-2 PSU in the northern and eastern parts [17].	Two levels were adopted: 5.0–5.5 PSU (coastal variant) and 7.0–7.2 PSU (open Baltic).
Water temperature	In summer, usually 15–20°C in the open Baltic Sea. In mid-winter, slightly below 0°C [23].	T_w from –0.5 to 20°C was used in the scenarios.
Ice season	Maximum ice cover usually occurs in January-March. In severe winters, ice may extend far to the south [15].	This justifies the BW-COLD case and range $T_{amb} = -20°C$.
Waves and storms	H_s values up to 7.8 m were observed in the Baltic Proper. Summer storms can produce H_s of about 4.1 m [18].	Sea states 1–6 were introduced in the scenarios and 0–7 in the additional analysis.
Frequency of wave events	In winter, H_s > 2.5 m occurs about once a week in larger sub-basins. H_s > 4 m occurs 1–2 times per month in the Baltic Proper [7].	The importance of the winter open-sea variant was therefore increased.
Sea-state scale	WMO Code 3700: states 3–7 correspond to H_s = 0.5–9 m [31].	Mid-range H_s values were used to translate sea state into vessel motions.

Based on the above range of conditions, 11 scenarios were defined. Eight of them concern the Baltic Sea and include four seasons and two exposure levels (coastal and open-sea variants). Two North Sea scenarios were retained as references with high chloride loading. One scenario, BW-MIT, represents the same environmental case as BW-STORM, but after implementation of a protection package: dehumidification, aerosol filtration, local heating, controlled humidification of the PEMFC/BOP section and modified dynamic tuning of the mounting. This enables comparison of the environmental influence on hybrid-system operation both with and without protective measures.

Table 2. Input data for model scenarios

ID	Short description	Season	T_{amb} [°C]	T_w [°C]	RH [%]	S_d [mg/(m²·d)]	U10 [m/s]	Sea state
BW-COLD	Coastal Baltic, winter, cold stand-still	win.	–20	–0.5	75	8	6	1
BW-STORM	Open Baltic, winter storm	win.	–10	1.0	90	120	22	6
BS-COAST	Coastal Baltic, spring	spr.	4	4.0	78	15	7	2
BS-OPEN	Open Baltic, spring	spr.	6	5.0	82	45	12	4
BL-COAST	Coastal Baltic, hot summer	sum.	25	20.0	76	12	5	2
BL-OPEN	Open Baltic, humid summer	sum.	22	18.0	85	55	12	4
BA-COAST	Coastal Baltic, autumn	aut.	10	12.0	88	25	10	3
BA-STORM	Open Baltic, autumn storm	aut.	8	10.0	94	110	18	5
NP-SUM	North Sea offshore, summer	sum.	18	14.0	90	380	15	5
NP-WIN	North Sea offshore, winter	win.	6	6.0	96	650	20	6
BW-MIT	BW-STORM with protection package	win.	–10	1.0	60	15	22	6

Note: T_{amb} denotes ambient temperature outside the hull, T_w denotes water temperature, RH is the relative humidity of local air in the compartment near the analyzed component, S_d is the annual chloride deposition rate according to the ISO 9223/9225 logic, and U10 is wind speed at 10 m above the sea surface.

The mean daily deposition rate S_d is not a measurement made on the vessel, but a scenario value consistent with the ISO 9223/9225 classification logic. In the adopted scenario set, values of 8–55 mg/(m²·d) correspond to class S1, values of 110–120 mg/(m²·d) to class S2, and the North Sea scenarios of 380–650 mg/(m²·d) to class S3 [20, 22].

3.2. Computational model

The proposed model is comparative in nature. The four modules comprising the model were selected based on their established physical or normative foundations, the availability of input data, and their ability to provide comparable scalar outputs. The modules describe, respectively, condensation risk, first-year atmospheric corrosion according to ISO 9223, PEMFC electrochemical losses, and the dynamic response to wave-induced excitation. They share a common scenario definition but remain physically independent. Their outputs are combined only after being normalized to dimensionless form. Therefore, the proposed framework constitutes a unidirectional comparative assessment rather than a fully coupled multiphysics model.

To assess condensation conditions, the local air temperature in the immediate vicinity of the device was described by the parameter T_{loc}. The component surface temperature T_{surf} was determined from a steady one-node heat balance, which includes heat exchange with the local air in the compartment, ambient air, seawater and the internal heat source $\dot{Q}_{op}$. In this formulation, the influence of reference temperatures follows directly from the equivalent thermal conductances $h_i A_i$, whereas the influence of device operation is explicitly included through the source term $\dot{Q}_{op}$ [17, 23, 36, 45].

$$T_{surf} = \frac{h_c \cdot A_c \cdot T_{loc} + h_a \cdot A_a \cdot T_{amb} + h_w \cdot A_w \cdot T_w + \dot{Q}_{op}}{h_c \cdot A_c + h_a \cdot A_a + h_w \cdot A_w} \quad (1)$$

where: T_{surf} – component surface temperature [°C], T_{loc} – local air temperature in the compartment near the component [°C], T_{amb} – ambient air temperature [°C], T_w – seawater temperature, h_c – heat-transfer coefficient between the surface and the local air in the compartment [W/(m^{2}K)], h_a – heat-transfer coefficient between the surface and ambient air[W/(m^{2}K)], h_w – heat-transfer coefficient between the surface and water, e.g. through the hull [W/(m^{2}K)], A_c, A_a, A_w – effective heat-transfer areas for the respective heat-exchange paths [m^2].

The dew point was determined using the Magnus equation in the Alduchov-Eskridge approximation [1]:

$$\gamma(T, RH) = \frac{a \cdot T_{air,loc}}{b + T_{air,loc}} + \ln\left(\frac{RH}{100}\right) \quad (2)$$

$$T_{dew} = \frac{b\gamma}{a - \gamma}, \quad a = 17.62, \quad b = 243.12°C \quad (3)$$

The condensation margin was defined as $\Delta T = T_{surf} - T_{dew}$ (dew point). A negative value indicates conditions favourable for moisture condensation on the coldest surfaces. In addition, on an annual or seasonal basis, the time of wetness can be described according to ISO 9223 as:

$$\tau = t(RH > 80\%, T > 0°C) \quad (4)$$

The lack of information on the temporal variability of RH and T made it impossible to determine tau in hours per year. In this paper, tau is treated as an indicator for future monitoring, whereas the scenario comparison is based on the condensation margin ΔT.

Chloride loading was determined from literature-based data. The annual chloride deposition rate S_d [mg/(m²·d)] was adopted as the input variable in accordance with the ISO 9223/9225 logic and atmospheric salinity classes S0-S3 [20, 22]. In this way, the environment was separated from the material corrosion response.

In practice, this means that the model directly selects the S_d level rather than using an intermediate multiplier based on salinity, wind and sea state. The corrosion part was based directly on the ISO 9223 dose-response function for carbon steel [20].

The ISO 9223 dose-response function enables determination of the first-year corrosion loss of carbon steel, expressed in µm/year. In this study, these values are presented in mm/year after conversion according to the following relationship:

$$r_{corr,mm} = \frac{r_{corr,\mu m}}{1000} \quad (5)$$

It should be emphasized that the obtained result is not a prediction of long-term durability. Such extrapolation would require the relationships described in ISO 9224 or validation under real exposure conditions [20, 21].

The relationship defining the corrosion loss has the form:

$$r_{corr} = 1.77\, P_d^{0.52} \exp(0.020 \cdot RH + f_{St}) + 0.102\, S_d^{0.62} \exp(0.033 \cdot RH + 0.040 \cdot T_{amb}) \quad (6)$$

where the temperature function is defined as:

$$f_{St} = \begin{cases} 0,150\,(T_{amb} - 10), & \text{for } T_{amb} \le 10°C \\ -0,054\,(T_{amb} - 10), & \text{for } T_{amb} > 10°C \end{cases} \quad (7)$$

In the above relationships, P_d denotes sulfur dioxide (SO_2) deposition [mg/(m²·d)]. In the calculations, P_d = 5 mg/(m²·d) was assumed for the Baltic scenarios and BW-MIT, and P_d = 6 mg/(m²·d) for the North Sea scenarios.

To represent the influence of water vapour on the operation of the PEMFC and its auxiliary systems (BOP), a classical relationship chain was adopted: water activity a_w determines the membrane water content λ, which in turn affects proton conductivity σ_m and, consequently, ohmic losses η_Ω. Activation losses described by the Tafel equation were also included [5, 6, 26, 32, 37]. As a first approximation, $a_w = RH/100$ was assumed, except for the BW-MIT variant, in which controlled humidification of the gas path was taken into account.

The membrane water content was determined using the empirical relationship:

$$\lambda(a_w) = 0.043 + 17.81 \cdot a_w - 39.85 \cdot a_w^2 + 36.0 \cdot a_w^3 \quad (8)$$

whereas proton conductivity was described by:

$$\sigma_m = (0.005139 \cdot \lambda - 0.00326) \cdot \exp\left[1268 \cdot \left(\frac{1}{303} - \frac{1}{T_{mem}}\right)\right] \quad (9)$$

Ohmic losses were determined from:

$$\eta_\Omega = \frac{i \cdot l_m}{\sigma_m} \quad (10)$$

where: η_Ω – ohmic loss (voltage drop caused by conduction resistance) [V], i – operating current density [A/cm²], l_m – membrane thickness [cm], σ_m – membrane proton conductivity [S/cm].

The additional activation loss was written in the classical Tafel form:

$$\eta_{act} = \frac{RT_{mem}}{\alpha \cdot n \cdot F} \cdot \ln\left(\frac{i}{i_0}\right) \quad (11)$$

where: η_{act} – activation loss [V], R – universal gas constant $R = 8{,}314\ J/(mol \cdot K)$, T_{mem} – membrane temperature [K], α – charge-transfer coefficient [–], n – number of electrons involved in the reaction [–], F – Faraday constant $F = 96485\ C/mol$, i – operating current density [A/cm²], i_0 – exchange current density [A/cm²].

The following parameter values were assumed in the calculations: $T_{mem} = 333.15\ K$, $i = 0.35\ A/cm^2$, $l_m = 125\ \mu m$, $\alpha = 0.5$, $n = 2$, $i_0 = 1 \cdot 10^{-6}\ A/cm^2$. In the presented formulation, the activation loss η_{act} is a reference component for the adopted constant values of i, i_0, α, n and T_{mem}. The scenario variability of the total electrochemical losses $\eta_\Omega + \eta_{act}$ results mainly from changes in effective water activity $a_{w,eff}$, membrane water content λ and conductivity σ_m.

The influence of salt aerosol on kinetic parameters(i_0) and transport parameters (σ_m) was not included directly in this model and requires separate experimental calibration based on electrochemical impedance spectroscopy (EIS) and polarization-curve analysis.

As a result, the electrochemical load was represented by the sum of losses $\eta_\Omega + \eta_{act}$, rather than by a separate contamination index for the PEMFC/BOP section. This approach enables distinguishing the influence of a humid-salt environment from the effects of insufficient hydration in the PEMFC/BOP system.

The dynamic part of the model was based on a classical seakeeping analysis chain, in which wave parameters, i.e. significant wave height H_s and zero-crossing period T_z, provide input data for constructing the wave spectrum. Then, through transformation to encounter frequency and the use of a response amplitude operator (RAO), the system response spectrum was obtained, from which the root mean square acceleration a_{rms} was calculated.

In accordance with ITTC recommendations for fetch-limited basins, which include the Baltic Sea, the JONSWAP spectrum was applied [16, 24] and described by the following relationship:

$$S_\zeta(\omega) = \alpha g^2 \omega^{-5} \exp\left[-1{,}25\left(\frac{\omega_p}{\omega}\right)^4\right]\gamma^r \quad (12)$$

$$r = \exp\left\{-\frac{(\omega/\omega_p - 1)^2}{2\sigma^2}\right\} \quad (13)$$

where: $S_\zeta(\omega)$ – wave energy density spectrum (free-surface spectrum) [m²·s], ω – wave angular frequency [rad/s], ω_p – angular frequency corresponding to the spectral maximum (peak frequency) [rad/s], α– spectrum scaling coefficient (wave-energy parameter), g – gravitational acceleration, γ – JONSWAP peak enhancement factor [-], r – peak-shape function defined as: $r = \exp\left\{-\frac{(\omega/\omega_p - 1)^2}{2\sigma^2}\right\}$, σ – peak-width parameter (usually taken as 0.07 for $\omega \le \omega_p$ and 0.09 for $\omega > \omega_p$).

For a vessel moving at non-zero speed, the wave spectrum should be transformed into the frequency domain observed on the vessel, i.e. encounter frequency:

$$\omega_e = \omega\left(1 - \frac{V\omega}{g}\cos\mu\right) \quad (14)$$

$$S_x(\omega_e) = |\,RAO(\omega_e)\,|^2\, S_\zeta(\omega_e), S_a(\omega_e) =$$
$$= \omega_e^4 S_x(\omega_e), a_{rms} = \left(\int S_a(\omega_e)\, d\omega_e\right)^{1/2} \quad (15)$$

In this analysis, standstill or low manoeuvring speeds were assumed, which allows the simplification $V \approx 0$ and $\omega_e \approx \omega$. The applied RAO is reduced in nature and is used only for scenario comparison. Full identification of the dynamic response would require detailed hydrodynamic calculations of the vessel hull or measured vessel-motion data.

In addition, the mounting response was described by the auxiliary transmissibility:

$$T_r = \left[\frac{1+(2\zeta r)^2}{(1-r^2)^2+(2\zeta r)^2}\right]^{1/2}, r = \frac{\omega_{dom}}{\omega_n} \quad (16)$$

where ζ denotes the damping ratio and ω_n is the natural frequency of the system.

The results of vessel-motion analysis are presented using the root mean square acceleration a_{rms}, whereas the mounting response is assessed using the mounting transmissibility T_r.

The final scenario assessment was carried out using the proposed decision metric:

$$R^* = 0.30\, C^* + 0.30\, K^* + 0.20\, E^* + 0.20\, D^* \quad (17)$$

where C*, K*, E* and D* denote the normalized values of condensation deficit, first-year corrosion loss, additional electrochemical load of the PEMFC/BOP section and dynamic response, respectively.

The following reference values were used for normalization (Table 3).

To limit the influence of extreme values, all normalized components were constrained to the interval [0, 1].

The baseline weights were not estimated from failure statistics and are not treated as universal material constants. They implement a transparent two-level prioritization: condensation and corrosion receive 0.30 each because they represent direct surface-wetting and material-loss mechanisms, whereas electrochemical and dynamic responses receive 0.20 each because their functional consequences depend more strongly on the operating point and component configuration. To prevent the ranking from depending on a single expert-selected vector, each weight was varied independently by ± 0.10, and the vector was then renormalized to unity in 5000 draws. The scientific interpretation is therefore based on the stability of the ranking over the admissible weight domain rather than on the exact values of one weight set. Once bench-test and operational data become available, the weights should be re-estimated using statistical or multicriteria calibration.

It should be emphasized that equation (17) is a decision metric for comparing scenarios. The quantity R* should not be interpreted as a probability of failure.

The scenario comparison and ranking (Fig. 2) constitute the final element of the model, whereas its physical part is based on established relationships in the literature [1, 5, 6, 16, 19–22, 24, 26, 32, 37].

The model is a parametric ranking tool, and its core has a literature basis: heat balance and dew point [1, 17, 23, 36, 45], the ISO 9223/9224 dose-response function [20, 21], the Springer relations and the Tafel equation [5, 6, 26, 32, 37], and JONSWAP/ITTC with RAO [16, 19, 24]. The model ultimately constructs the decision metric R*, while uncertainty arises mainly from the adopted scenario assumptions and the simplifications used to represent real operating conditions.

Table 3. Reference values used for normalization

Symbol	Physical quantity	Meaning	Normalization method	Reference value
C*	Condensation deficit ΔT	Describes the tendency to moisture condensation. Negative values indicate conditions favourable for condensation.	$C^* = \min\left(\frac{\max(0, -\Delta T)}{6}, 1\right)$	6°C
K*	Corrosion loss r_{corr}	Intensity of the corrosive environmental effect (first-year corrosion loss).	$K^* = \min\left(\frac{r_{corr}}{0.18}, 1\right)$	0.18 mm/year
E*	Excess electrochemical losses $\Delta\eta$	Additional PEMFC/BOP load relative to the reference case.	$E^* = \min\left(\frac{\Delta\eta}{120}, 1\right)$	120 mV
D*	Dynamic response a_{rms}	Level of dynamic excitation acting on the system.	$D^* = \min\left(\frac{a_{rms}}{3}, 1\right)$	3.0 m/s²

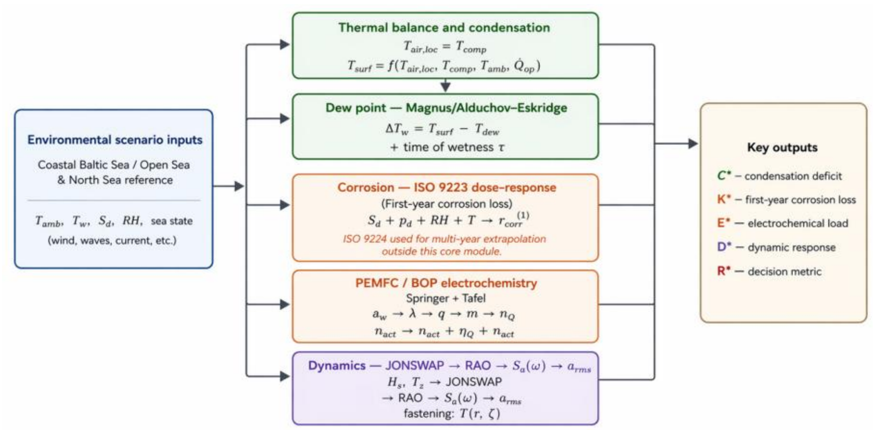

Fig. 2. Computational framework and decision metric

Table 4. Main uncertainty sources and working ranges

Model block	Main parameters/equations	Uncertainty and working range	Dominant influence
Heat balance and condensation	T_{comp}, $h_c \cdot A_c$, $h_a \cdot A_a$, $h_w \cdot A_w$, RH	$T_{surf} \pm 2°C$, RH $\pm$ 5 p.p.	condensation margin ΔT
Chloride deposition S_d	S_d, S0–S3 class, exposure scenario	seasonal variability, $S_d \pm 25 - 40\%$	ISO 9223 corrosion block
ISO 9223 corrosion	P_d, S_d, RH, T	first-year corrosion loss. Not directly applicable to long-term durability	material-part ranking
PEM Springer/Tafel	$a_{w,eff}$, λ, σ_m, i_0	$a_w \pm 0{,}05$, $l_m \pm 10\%$, $i_0 \times/\div 2$	$\eta_\Omega + \eta_{act}$, and assessment of the PEM/BOP section
JONSWAP/RAO dynamics	T_z, H_s, f_n, ζ	highest sensitivity at the dominant response frequency and when changing mounting tuning	a_{rms} and position relative to resonance
Decision metric	w_C, w_K, w_E, w_D	expert selection (each weight +/-0.10)	R* ranking

The ranges presented in Table 4 are indicative and are used to assess model sensitivity. They should not be treated as confidence intervals. The model shows the highest sensitivity near limiting values, i.e. for $\Delta T \approx 0°C$, at transitions between S_d classes and near the dominant dynamic-response frequency. This means that, in these regions, even small changes in input parameters may lead to a clear change in the result. Therefore, the interpretation of results should be based primarily on trend analysis and on the assessment of safety margins.

4. Results

4.1. Temperature cases

The influence of seasonal variability in environmental conditions on the model results is presented below. The analysis was carried out for four characteristic temperature cases corresponding to winter, spring, summer and autumn. The results shown in Fig. 3 indicate that accounting for seasonality enables separation of two important mechanisms: the risk of moisture condensation and the effect of humidity conditions on PEMFC membrane hydration.

The BW-COLD variant retains a positive condensation margin of ΔT = 1.8°C, despite the ambient temperature falling to –20°C. This means that low temperatures, combined with low air humidity, do not necessarily lead to condensation on the coldest surfaces. At the same time, the same variant is unfavourable from the membrane-operation point of view, because dry conditions reduce its hydration and translate into higher electrochemical losses $\eta_\Omega + \eta_{act}$.

The most unfavourable Baltic case with respect to condensation is BW-STORM, for which $\Delta T = -4.8°C$ was obtained. The negative condensation margin indicates conditions conducive to moisture deposition on the coldest surfaces. In the entire analyzed set, the highest material-moisture load occurs in the NP-WIN scenario, for which $\Delta T = -3.3°C$ together with much higher chloride deposition S_d.

The BA-STORM variant is a transitional but still demanding case because it combines a small condensation deficit with a high wetting level and an unfavourable sea state. In turn, BL-OPEN does not exhibit a clear condensation deficit but remains close to the condensation boundary. This means that summer conditions should not automatically be treated as safe, especially when high humidity, salt aerosol and dynamic effects occur simultaneously.

The analysis also included the influence of marine salt on the system under investigation. Figure 4 compares three key environmental loads: chloride deposition S_d, corrosion loss r_{corr} and electrochemical losses $\eta_\Omega + \eta_{act}$, showing their different effects on the analyzed propulsion system. The highest chloride loading occurs in the North Sea scenarios: NP-SUM ($S_d = 380\ mg/(m^2 \cdot d)$) and NP-WIN (650 mg/(m²·d)). In the Baltic Sea, the highest values were adopted for BW-STORM (120 mg/(m²·d)) and BA-STORM (110 mg/(m²·d)), which is consistent with open-sea exposure and storm episodes.

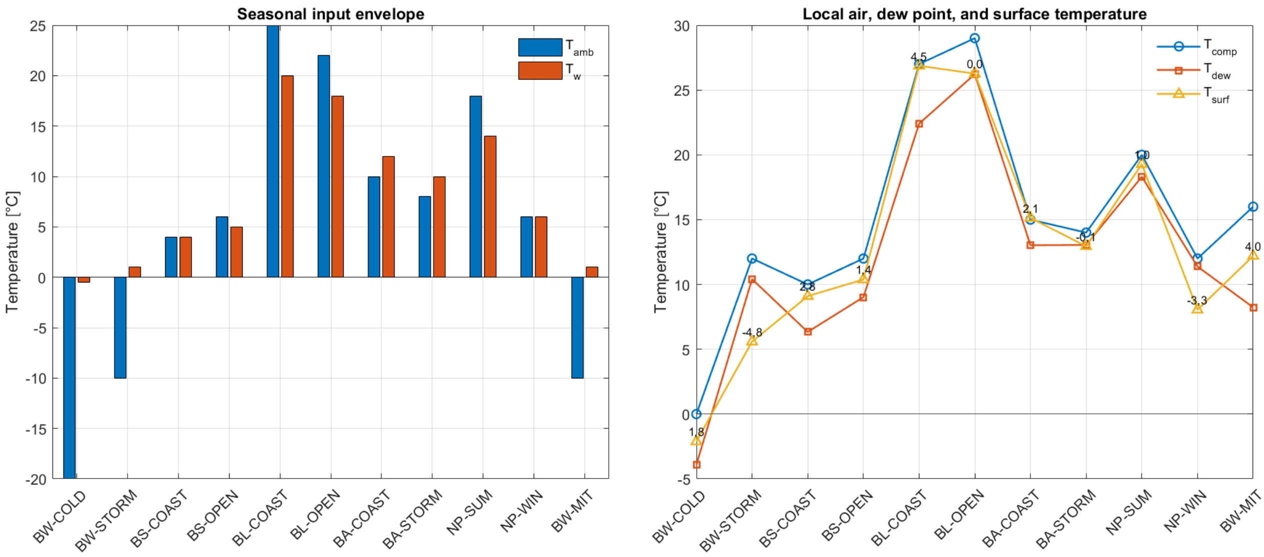

Fig. 3. Seasonal thermal and condensation results ΔT

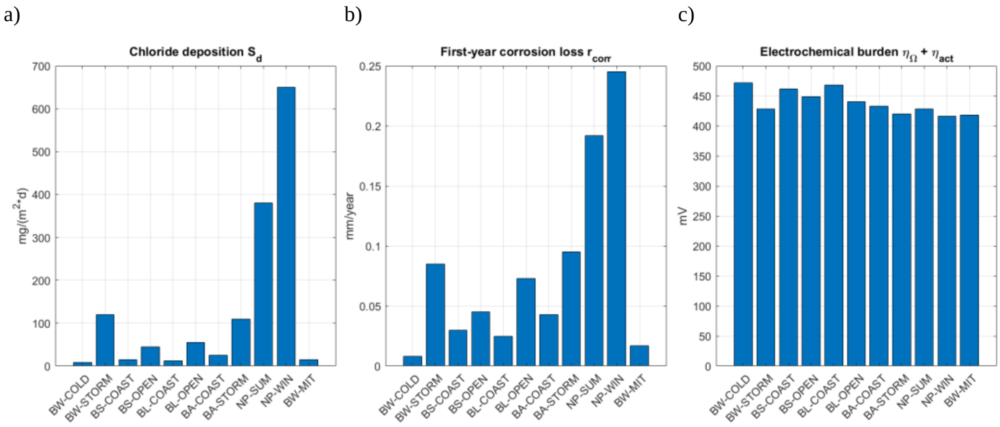

Fig. 4. Environmental and electrochemical response of the analysed scenarios: a) chloride deposition, b) first-year corrosion loss, c) PEMFC/BOP electrochemical load

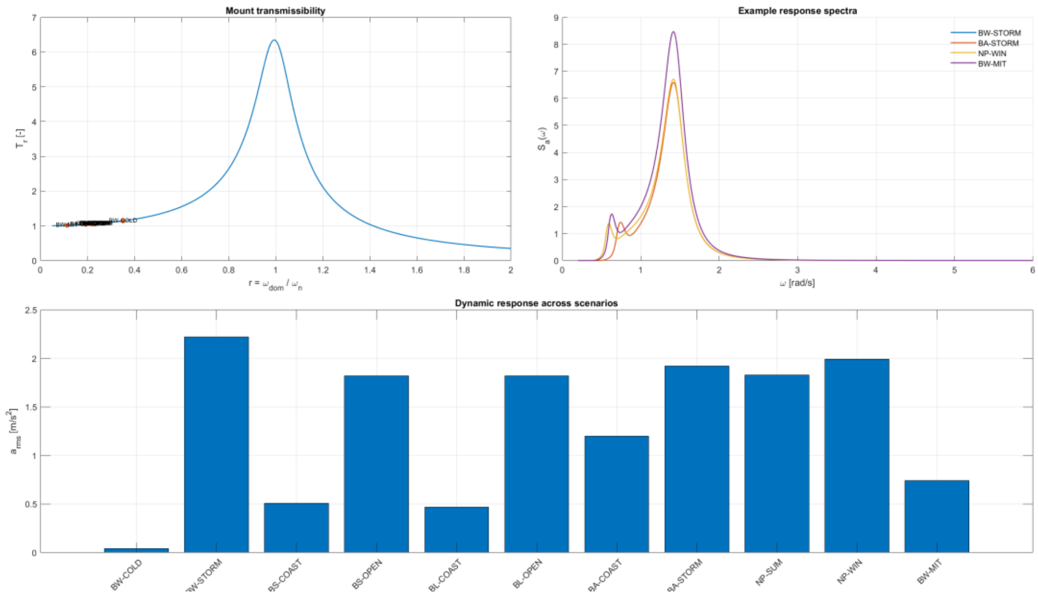

Fig. 5. Dynamic response and mounting transmissibility

After applying the ISO 9223 relationships, the highest first-year corrosion losses were obtained for the North Sea scenarios, i.e. NP-WIN ($r_{corr} = 0.245$ mm/year) and NP-SUM ($r_{corr} = 0.192$ mm/year). Within the Baltic Sea, the most unfavourable material case is BA-STORM (0.095 mm/year), slightly ahead of BW-STORM (0.085 mm/year). These results are clear to interpret because the corrosion module is based directly on the environmental parameters S_d, P_d, RH and T, without additional arbitrary coefficients. Consequently, the relationships obtained directly link changes in environmental parameters with the intensity of corrosion processes.

The part related to PEMFC/BOP operation exhibits a different behaviour. The highest values of total electrochemical losses $\eta_\Omega + \eta_{act}$ were obtained for BW-COLD (471.7 mV) and BL-COAST (468.2 mV), i.e. for relatively low-humidity cases rather than for scenarios with the highest chloride loading. This indicates that separating the models reveals two distinct risk mechanisms: a humid-salt environment intensifies corrosion, whereas overly dry conditions lead to insufficient membrane hydration and increase the electrochemical load on the PEMFC/BOP section.

4.2. Influence of waves

This subsection analyzes the influence of wave conditions on the system's dynamic response, considering the progression from the wave spectrum to the loads acting on the mounting. Figure 5 shows that, after applying the calculation algorithm consisting of the JONSWAP spectrum, the RAO response operator and mounting parameters, the system dynamic response can be clearly characterized by the root mean square acceleration a_{rms}, whereas the transmissibility T_r acts as an interpretative indicator of the system position relative to the resonance region. For the baseline mounting settings, T_r values fall within the narrow range of 1.04–1.06, which indicates no significant amplification by the isolator itself. Consequently, the dynamic load level is determined primarily by the hull response spectrum.

The highest a_{rms} values were obtained for BW-STORM (2.22 m/s²) and NP-WIN (1.99 m/s²), whereas BA-STORM (1.92 m/s²) corresponds to the second, autumn maximum of dynamic loads. Changing the mounting tuning in BW-MIT leads to a significant reduction in dynamic response, expressed by a decrease in a_{rms} to 0.74 m/s² and a simultaneous reduction of transmissibility to $T_r = 1.01$, indicating that the system has moved away from resonance conditions.

Based on the obtained results, the sea state should first be represented as a wave spectrum and the corresponding structural response spectrum, and only then be transformed into loads acting on the mounting system. This approach better reflects the physical mechanism of dynamic-load generation than a direct transition from the sea-state scale to a single assessment indicator.

4.3 Decision metric and scenario ranking

The analysis includes an integrated assessment of the scenarios using the R* metric, which accounts for four main factors: condensation, first-year corrosion loss, electrochemical loading of the PEMFC/BOP section and system dynamic response.

The results presented in Fig. 6 and Table 5 show that the most unfavourable scenarios are not caused by a single factor but by the simultaneous overlap of several environmental mechanisms. The highest index value in the whole analyzed set was obtained for NP-WIN (R* = 0.60), whereas among the Baltic scenarios the highest load level was reached by BW-STORM (R* = 0.55). The next Baltic case is BA-STORM (R* = 0.30), while BS-OPEN and BL-OPEN form a moderate class, with R* = 0.25 and R* = 0.28, respectively.

Introducing the BW-MIT variant leads to a substantial reduction in load relative to BW-STORM. The R* metric decreases by 86.5%, corrosion loss r_{corr} by 79.5%, the sum of electrochemical losses $\eta_\Omega + \eta_{act}$ by 2.4%, and the dynamic response a_{rms} by 66.5%. The results indicate that, after separating the PEMFC/BOP model from the chloride indicator, the protection package acts primarily by eliminating condensation-favouring conditions, reducing chloride deposition and decreasing the dynamic response of the system.

The reported values are relative outputs of the scenario model and apply only to the adopted inputs and assumptions. They do not represent failure probabilities, certification thresholds or lifetime predictions. The ranking is intended solely for prioritization and requires validation before application to other vessels or exposure conditions.

The small improvement in electrochemical load results from the assumption of controlled humidification of the PEMFC/BOP section in BW-MIT. This means that the effectiveness of this variant is not related solely to reducing the humid-salt environmental impact, but also to improving membrane operating conditions and obtaining a more favourable dynamic-response configuration.

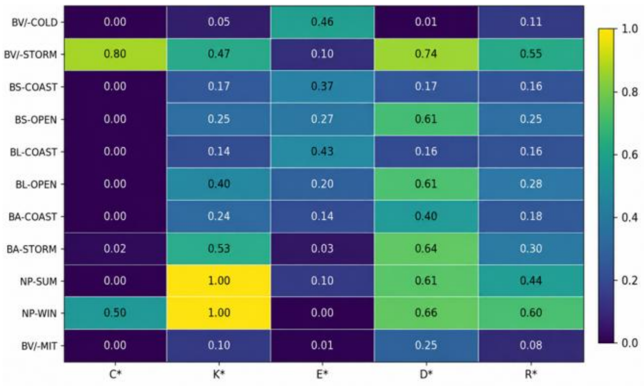

Fig. 6. Normalized components and final decision metric R*

Relative classes were introduced solely for within-study interpretation: low for $R^* < 0.20$, moderate for $0.20 \le R^* < 0.40$, high for $0.40 \le R^* < 0.55$, and very high for $R^* \ge 0.55$. These classes are not reliability or failure-probability categories.

4.4 Sensitivity test of the R* index weights

Because of the adopted choice of weights used in equation (17), a sensitivity analysis of the R* metric was performed. For this purpose, 5000 variants of the weight vector were generated within ±0.10 of the baseline values [0.30; 0.30; 0.20; 0.20], and each set was then normalized so that the sum of weights was equal to one. The calculations were performed for the previously determined components C*, K*, E* and D*.

Table 5. Scenario results and R* ranking

ID	T_{dew} [°C]	T_{surf} [°C]	ΔT [°C]	S_d [mg/(m²·d)]	r_{corr} [mm/year]	$\eta_\Omega + \eta_{act}$ [mV]	a_{arm} [m/s²]	$R*$ [–]	Relative R^*class
BW-COLD	–3.9	–2.1	1.8	8	0.008	471.7	0.04	0.11	low
BW-STORM	10.4	5.6	–4.8	120	0.085	428.5	2.22	0.55	very high
BS-COAST	6.3	9.1	2.8	15	0.030	461.4	0.51	0.16	low
BS-OPEN	9.0	10.4	1.4	45	0.045	449.0	1.82	0.25	moderate
BL-COAST	22.4	26.9	4.5	12	0.025	468.2	0.47	0.16	low
BL-OPEN	26.2	26.3	0.0	55	0.073	440.6	1.82	0.28	moderate
BA-COAST	13.0	15.1	2.1	25	0.043	433.1	1.20	0.18	low
BA-STORM	13.0	12.9	–0.1	110	0.095	420.3	1.92	0.30	moderate
NP-SUM	18.3	19.3	1.0	380	0.192	428.5	1.83	0.44	high
NP-WIN	11.4	8.1	–3.3	650	0.245	416.6	1.99	0.60	very high
BW-MIT	8.2	12.2	4.0	15	0.017	418.4	0.74	0.08	low

The aim of the analysis was not to identify a single optimal set of weights, but to assess the stability of the scenario ranking under changes in the adopted weighting assumptions. This approach makes it possible to check whether the obtained scenario ranking results from real differences between cases or is strongly dependent on arbitrary weight selection in the decision metric.

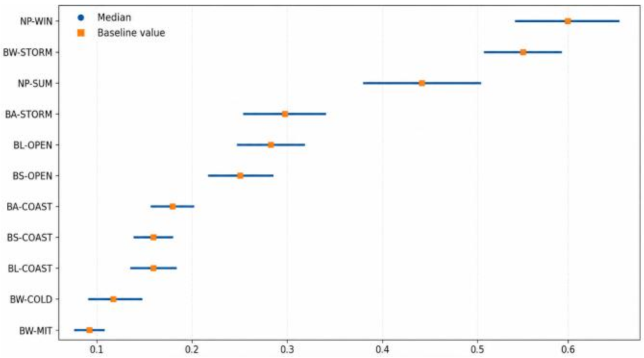

Fig. 7. Sensitivity of R* to the choice of weights

Figure 7 shows that the range of R* variability remains limited and that the scenario ranking is stable. NP-WIN retains the highest R* values in the whole set, whereas BW-STORM remains the most unfavourable Baltic scenario. Additional frequency analysis showed that NP-WIN ranked first globally in 91.2% of draws, and BW-STORM ranked first among Baltic scenarios in 100% of draws.

In summary, the adopted metric shows high robustness to changes in the weighting assumptions, and the conclusions are stable from an engineering-interpretation point of view.

5. Discussion

5.1. Environmental loads and propulsion system readiness

The results presented show that the Baltic Sea cannot be treated solely as a milder equivalent of the North Sea. Although the lower chloride deposition S_d reduces first-year corrosion loss, a suitable combination of relative humidity and sea state may cause open-Baltic conditions, especially in winter, to generate a high level of total environmental load. From the vessel's perspective, it is therefore important not to rely on a single averaged environmental characteristic, but to distinguish among coastal variants, open-sea conditions, and storm episodes.

An important methodological element of the model is the separation of salinity effects from the description of PEMFC/BOP operation. In the adopted formulation, chloride deposition S_d acts directly on the ISO 9223 corrosion module, whereas the membrane section is described through membrane hydration, proton conductivity and activation losses. This approach avoids the need for poorly calibrated intermediate indicators, and the impact of the marine environment on the PEMFC/BOP section is interpreted primarily indirectly – through humidity conditions, deposits in flow paths, the quality of working media and degradation of BOP auxiliary-system elements.

A similar structuring was introduced in the dynamic part of the model. Instead of directly linking the sea-state scale with the risk level, the following classical calculation chain was applied:

$$H_s,\ T_z \rightarrow \text{JONSWAP spectrum} \rightarrow \text{RAO} \rightarrow a_{rms}$$

whereas the mounting response was described using the known transmissibility relationship $T_r(r,\zeta)$ for base excitation. This approach clearly separates the environmental description from the object characteristics and thereby facilitates interpretation of the dynamic response.

The selected literature confirms the model's usefulness for interpreting processes in the PEM section, particularly transient phenomena and the influence of ambient temperature [2, 3, 11–13, 42–45]. At the same time, the model core is based on standards and classical calculation relationships, which increases its transparency, repeatability and potential for independent verification.

From the propulsion-system operation perspective, the key issue is translating the environmental-analysis results into system functioning. Variants characterized by high chloride deposition S_d and a negative condensation margin do not only imply accelerated surface corrosion. In practice, they may also reduce the readiness of the PEMFC/BOP section to cover peak power demand, destabilize gas and air preparation processes, increase the risk of measurement errors and accelerate degradation of connectors and cables. Conversely, variants with relatively low humidity, despite limited corrosion effects, may increase electrochemical losses $\eta_\Omega + \eta_{act}$, which reduces system efficiency without a simultaneous increase in corrosion rate.

Table 6. Transfer of environmental mechanisms to propulsion function and readiness

Environmental mechanism	Propulsion-system element	Functional effect
Condensation on cold surfaces	Connectors, harnesses, sensors, air ducts	Increased leakage current, diagnostic errors and longer start-up time
Chloride deposition and corrosion	Enclosures, heat exchangers, pipes, BOP fittings	Loss of tightness, increased flow resistance and higher maintenance demand
Unfavourable membrane hydration and increased ohmic resistance	PEMFC stack and gas/air path	Increase in $\eta_\Omega + \eta_{act}$, voltage drop, limitation of auxiliary-source power
Vibrations and proximity to the dominant response frequency	Mountings, power-electronics cabinets, and connectors	Connection loosening, material fatigue, protection trips, reduced availability

This linkage indicates that the proposed ranking should not be interpreted as an assessment of corrosion alone, but rather as a preliminary tool for evaluating the propulsion system's energy and maintenance readiness. In design practice, simultaneous monitoring of the four partial components is recommended because the metric acts as a decision indicator and not as a measure of failure probability.

5.2. Model assumptions, limitations and validation

The present framework is intended for preliminary comparative qualification. The thermal block uses a steady one-node balance and does not resolve spatial temperature gradients, transient heat storage or local airflow. The ISO 9223 module estimates first-year atmospheric corrosion loss and does not directly represent long-term degradation, splash-zone exposure or sheltered microclimates without additional calibration.

The PEMFC module uses effective water activity as a scenario variable and does not explicitly quantify salt-induced changes in exchange current density, membrane conductivity, catalyst-layer transport or BOP contamination. The dynamic module uses a reduced RAO and assumes standstill or low manoeuvring speed. It therefore does not replace vessel-specific six-degree-of-freedom hydrodynamic and structural calculations. The R^*metric has not been calibrated against failure or maintenance data and should be interpreted solely as a ranking tool.

Validation should combine onboard measurements of local air temperature, relative humidity, surface temperature and chloride deposition with cyclic salt-spray/RH–T testing, polarization curves and EIS, and vibration tests driven by measured vessel-motion spectra. Such data would allow calibration of scenario inputs, verification of the individual submodels and future data-based estimation of the R^*weights.

6. Conclusions

This study analyzed the influence of environmental conditions on the operation of a hybrid propulsion system across diverse operating scenarios. The approach made it possible to assess thermal-moisture, corrosion, electrochemical and dynamic effects in a multi-variant framework. The main conclusions are as follows:

1. Extending the Baltic analysis to four seasons and two exposure levels makes it possible to distinguish dry, humid and storm scenarios that are not captured by an averaged approach.
2. Under Baltic conditions, the highest load level occurs for BW-STORM (open Baltic, winter storm).
3. In the whole set, the highest index value is reached by NP-WIN, whereas in the Baltic Sea another important case is BA-STORM. This confirms the need to analyze multiple scenarios rather than a single averaged case.
4. Low temperature does not automatically imply a high condensation risk: BW-COLD retains a positive condensation margin ΔT, but at the same time it increases electrochemical load because of insufficient hydration.
5. The maxima of corrosion loss and electrochemical losses do not coincide: the humid-salt environment dominates corrosion, whereas dry conditions deteriorate membrane operation.
6. BW-MIT significantly reduces R*, confirming the effectiveness of dehumidification, filtration and mounting tuning. The ranking remains stable despite changes in the weights.
7. Further work should include S_d, measurements, salt-spray tests, dynamic testing, EIS measurements and CFD calculations, in order to partially validate the model.

The results indicate that the environmental load on the system arises from the combined effects of several environmental factors. Humid and saline conditions primarily intensify corrosion processes, whereas dry conditions may adversely affect the performance of the PEMFC/BOP section. The analysis of protective measures across multiple scenarios indicates the potential to reduce these loads and identifies directions for further research and partial experimental validation of the model.

The reported values should be interpreted as comparative outputs of the scenario-based model rather than predictions of component lifetime, reliability, or failure probability.

Nomenclature

BOP	balance of plant
EIS	electrochemical impedance spectroscopy
FC	fuel cell
FMI	Finnish Meteorological Institute
HELCOM	Helsinki Commission
ISO	International Organization for Standardization
ITTC	International Towing Tank Conference
JONSWAP	Joint North Sea Wave Project wave spectrum
MEA	membrane electrode assembly
PEM	proton exchange membrane
PEMFC	proton exchange membrane fuel cell
PSU	practical salinity unit
RAO	response amplitude operator
RH	relative humidity
SO_2	sulfur dioxide
WMO	World Meteorological Organization

Bibliography

[1] Alduchov OA, Eskridge RE. Improved magnus form approximation of saturation vapor pressure. J Appl Meteorol. 1996;35(4):601-609. https://doi.org/10.1175/1520-0450(1996)035<0601:IMFAOS>2.0.CO;2

[2] Andrych-Zalewska M, Chłopek Z, Lasocki J, Merkisz J, Pielecha J. A stochastic approach to the analysis of pollutant emissions and fuel consumption of motor vehicles driven in real traffic. Appl Sci. 2024;14(23):11346. https://doi.org/10.3390/app142311346

[3] Andrych-Zalewska M, Chłopek Z, Merkisz J, Pielecha J. Exhaust emission from a vehicle engine operating in dynamic states and conditions corresponding to real driving. Combustion Engines. 2019;178(3):99-105. https://doi.org/10.19206/CE-2019-317

[4] Bampaou M, Georgiou D, Papaioannou K, Panopoulos KD. Post-mortem analysis as a method to identify degradation of PEM fuel cells affecting their durability in maritime applications. Int J Hydrogen Energy. 2025;177:151574. https://doi.org/10.1016/j.ijhydene.2025.151574

[5] Barbir F. PEM fuel cells: theory and practice. 2nd ed. Academic Press; 2012. https://shop.elsevier.com/books/pem-fuel-cells/barbir/978-0-12-387710-9

[6] Bard AJ, Faulkner LR. Electrochemical methods: fundamentals and applications. 2nd ed. Wiley; 2001. https://search.worldcat.org/title/471679025

[7] Björkqvist J-V, Kanarik H, Tuomi L, Niskanen L, Kankainen M. Event-based wave statistics for the Baltic Sea. State of the Planet. 2024;4-osr8:10. https://doi.org/10.5194/sp-4-osr8-10-2024

[8] Broer A, Polinder H, van Biert L. Polymer electrolyte membrane fuel cell degradation in ships: review of degradation mechanisms and research gaps. J Power Sources. 2025;640: 236678. https://doi.org/10.1016/j.jpowsour.2025.236678

[9] Choi H, Choi H, Choi HJ, Kim J, Kim O-H, Kim Y et al. Polymer electrolyte membrane fuel cell durability test using ship operation profile: a comparative study with durability test protocols. J Power Sources. 2025;632:236396. https://doi.org/10.1016/j.jpowsour.2025.236396

[10] Dall'Armi C, Pivetta D, Taccani R. Hybrid PEM fuel cell power plants fuelled by hydrogen for improving sustainability in shipping: state of the art and review on active projects. Energies. 2023;16(4):2022. https://doi.org/10.3390/en16042022

[11] Dudek M, Lis B, Raźniak A, Krauz M, Kawalec M. Selected aspects of designing modular PEMFC stacks as power sources for unmanned aerial vehicles. Appl Sci. 2021;11(2): 675. https://doi.org/10.3390/app11020675

[12] Dudek M, Raźniak A, Rosół M, Siwek T, Dudek P. Design, development, and performance of a 10 kW polymer exchange membrane fuel cell stack as part of a hybrid power source designed to supply a motor glider. Energies. 2020; 13(17):4393. https://doi.org/10.3390/en13174393

[13] Dudek M, Zarzycki M, Raźniak A, Rosół M. Applying a 2 kW polymer membrane fuel-cell stack to building hybrid power sources for unmanned ground vehicles. Energies. 2023;16(22):7531. https://doi.org/10.3390/en16227531

[14] Filina-Dawidowicz L, Filin S, Wojnicz L, Miłek D, Grzelak P. Energy-efficient maritime transport of refrigerated containers. Procedia Comput Sci. 2022;207:3572-3581. https://doi.org/10.1016/j.procs.2022.09.416

[15] Finnish Meteorological Institute. Ice season in the Baltic Sea. Helsinki: FMI; accessed 18 Apr 2026. https://en.ilmatieteenlaitos.fi/ice-season-in-the-baltic-sea

[16] Hasselmann K, Barnett TP, Bouws E, Carlson H, Cartwright DE, Enke K et al. Measurements of wind-wave growth and swell decay during the Joint North Sea Wave Project (JONSWAP). Ergänzungsheft zur Deutschen Hydrographischen Zeitschrift, Reihe A(8) Nr. 12. Hamburg: Deutsches Hydrographisches Institut; 1973. https://repository.tudelft.nl/record/uuid:f204e188-13b9-49d8-a6dc-4fb7c20562fc

[17] HELCOM. About the Baltic Sea. State of the Baltic Sea 2023. Helsinki Commission; 2023. https://stateofthebalticsea.helcom.fi/overview/about-the-baltic-sea/

[18] HELCOM. Wave climate in the Baltic Sea 2023 (BSEFS). Helsinki Commission; 2024. https://helcom.fi/publications/wave-climate-in-the-baltic-sea-2023/

[19] Inman DJ. Engineering Vibration. 4th ed. Pearson; 2014. https://uk.mathworks.com/academia/books/engineering-vibration-inman.html

[20] ISO 9223:2012. Corrosion of metals and alloys – Corrosivity of atmospheres – Classification, determination and estimation. Geneva: International Organization for Standardization; 2012. https://www.iso.org/standard/53499.html

[21] ISO 9224:2012. Corrosion of metals and alloys – Corrosivity of atmospheres – Guiding values for the corrosivity categories. Geneva: International Organization for Standardization; 2012. https://www.iso.org/standard/53500.html

[22] ISO 9225:2012. Corrosion of metals and alloys - Corrosivity of atmospheres – Measurement of environmental parameters affecting corrosivity of atmospheres. Geneva: International Organization for Standardization; 2012. https://www.iso.org/standard/53501.html

[23] Itämeri.fi. Water temperature – The Baltic Sea. Finnish Environment Institute/Finnish Meteorological Institute; accessed 18 Apr 2026. https://itameri.fi/en/the-baltic-sea-now/water-quality/water-temperature/

[24] ITTC. Seakeeping Experiments. Recommended Procedures and Guidelines 7.5-02-07-02.1. 2024 Revision 08. International Towing Tank Conference; 2024. https://ittc.info/downloads/quality-systems-manual/

[25] Kozak M, Chmiel J. Cold ironing galvanic corrosion issues with regard to a shore-to-ship medium voltage connection. Energies. 2020;13(20):5372. https://doi.org/10.3390/en13205372

[26] Larminie J, Dicks A. Fuel Cell systems explained. 2nd ed. Wiley; 2003. https://doi.org/10.1002/9781118878330

[27] Leo TJ, Durango JA, Navarro E. Exergy analysis of PEM fuel cells for marine applications. Energy. 2010;35(2):1164-1171. https://doi.org/10.1016/j.energy.2009.06.010

[28] Li S, Zhu J, Yang G, Shen Q. A review on impact of the marine salt spray environment on the performance of proton exchange membrane fuel cells. J Mar Sci Eng. 2025;13(1): 172. https://doi.org/10.3390/jmse13010172

[29] Lim J, Koo J, Shim JH. Failure modes of polymer electrolyte membrane fuel cell membrane-electrode assemblies in air-independent applications. Case Stud Therm Eng. 2025; 76:107455. https://doi.org/10.1016/j.csite.2025.107455

[30] McCay K, Karstensen PEE, Gerhardt M, Coolegem J, Damiano D, Lædre S. An analysis of the reversible and irreversible degradation of a PEM fuel cell short-stack operated under simulated maritime conditions. J Power Sources. 2026; 665:239011. https://doi.org/10.1016/j.jpowsour.2025.239011

[31] NOAA NCEI. WMO Code Table 3700: Sea State. National Oceanographic Data Center; accessed 18 Apr 2026. https://www.ncei.noaa.gov/access/world-ocean-database/CODES/s_18_sea_state.html

[32] O'Hayre R, Cha SW, Colella W, Prinz FB. Fuel Cell Fundamentals. 3rd ed. Wiley; 2016. https://doi.org/10.1002/9781119191766

[33] Radica G, Tolj I, Nyamsi SN, Vidović T. Performances of proton exchange membrane fuel cells in marine application. Int J Hydrogen Energy. 2025;142:186-194. https://doi.org/10.1016/j.ijhydene.2025.05.289

[34] Rostrup-Nielsen JR, Rostrup-Nielsen T. Reforming hydrocarbons for fuel cells. Springer 2011. https://doi.org/10.1016/B978-0-444-53563-4.10004-5

[35] Singheiser L, Huczkowski P, Markus T, Quadakkers WJ. High temperature corrosion issues for metallic materials in solid oxide fuel cells. In: Shreir's Corrosion. Elsevier 2010: 482-517. https://doi.org/10.1016/B978-044452787-5.00024-X

[36] Socik P. Analysis of the impact of the marine environment on components of the hybrid propulsion system of a project 207M vessel. Gdynia: Polish Naval Academy; 2024.

[37] Springer TE, Zawodzinski TA, Gottesfeld S. Polymer electrolyte fuel cell model. J Electrochem Soc. 1991;138(8): 2334-2342. https://doi.org/10.1149/1.2085971

[38] Tamburello S, Cirillo MR, Yakovlev Y, Matolínová I, Taccani R, Coraddu A et al. Preliminary methodology assessment for PEMFC durability testing in transport applications. Electrochim Acta. 2026;554:148267. https://doi.org/10.1016/j.electacta.2026.148267

[39] Van Hoecke L, Laffineur L, Campe R, Perreault P, Verbruggen SW, Lenaerts S. Challenges in the use of hydrogen for maritime applications. Energy Environ Sci. 2021;14:815-843. https://doi.org/10.1039/D0EE01545H

[40] Wen X, Zhu D, Hnydiuk-Stefan A, Ma Z, Królczyk G, Li Z. Energy storage performance of hydrogen fuel cells operating in a marine salt spray environment using experimental evaluation. Int J Hydrogen Energy. 2024;52:213-225. https://doi.org/10.1016/j.ijhydene.2023.03.400

[41] Xing H, Stuart C, Spence S, Chen H. Fuel cell power systems for maritime applications: progress and perspectives. Sustainability. 2021;13(3):1213. https://doi.org/10.3390/su13031213

[42] Zacharewicz M, Bogdanowicz A, Socik P. Capacitance-based assessment of water content in fuels and lubricating oils for marine engines. Combustion Engines. 2025;202(3): 81-87. https://doi.org/10.19206/CE-204692

[43] Zadrąg R, Socik P, Kniaziewicz T, Zacharewicz M, Bogdanowicz A, Wirkowski P. Analysis of simulated dynamic loads of a ship propulsion system of a non-conventional power system. Combustion Engines. 2024;197(2):158-168. https://doi.org/10.19206/CE-184139

[44] Zimakowska-Laskowska M, Kniaziewicz T. Analysis of methods for estimating pollutant emissions from marine engines in terms of their use for evaluating ambient air quality. Combustion Engines. 2025;202(3):3-10. https://doi.org/10.19206/CE-204922

[45] Zimakowska-Laskowska M, Kozłowski E, Wiśniowski P, Żbik K, Świderski A, Rostek E et al. The influence of ambient temperature on exhaust emissions during cold start in the homologation test. Combustion Engines. 2025;203(4):50-58. https://doi.org/10.19206/CE-207577

Paweł Socik, MEng. – Faculty of Mechanical and Electrical Engineering, Polish Naval Academy, Poland.
e-mail: *p.socik@amw.gdynia.pl*

Prof. Tomasz Kniaziewicz, DSc., DEng. – Faculty of Mechanical and Electrical Engineering, Polish Naval Academy, Poland.
e-mail: *t.kniaziewicz@amw.gdynia.pl*

Prof. Ryszard Zadrąg, DSc., DEng. – Faculty of Mechanical and Electrical Engineering, Polish Naval Academy, Poland.
e-mail: *r.zadrag@amw.gdynia.pl*

Paweł Wirkowski, DSc., DEng. – Faculty of Mechanical and Electrical Engineering, Polish Naval Academy, Poland.
e-mail: *p.wirkowski@amw.gdynia.pl*

Prof. Marcin Zacharewicz, DSc., DEng. – Faculty of Mechanical and Electrical Engineering, Polish Naval Academy, Poland.
e-mail: *m.zacharewicz@amw.gdynia.pl*

Adriana Włóka, MEng. – Faculty of Mechanical Engineering, Wrocław University of Science and Technology, Poland.
e-mail: *adriana.wloka@pwr.edu.pl*

Artur Bogdanowicz, DEng. – Faculty of Mechanical and Electrical Engineering, Polish Naval Academy, Poland.
e-mail: *a.bogdanowicz@amw.gdynia.pl*